Volume 20 | Number 23 | 7 December 2018 | Pages 5237–5406

Green Chemistry

Cutting-edge research for a greener sustainable future

rsc.li/greenchem

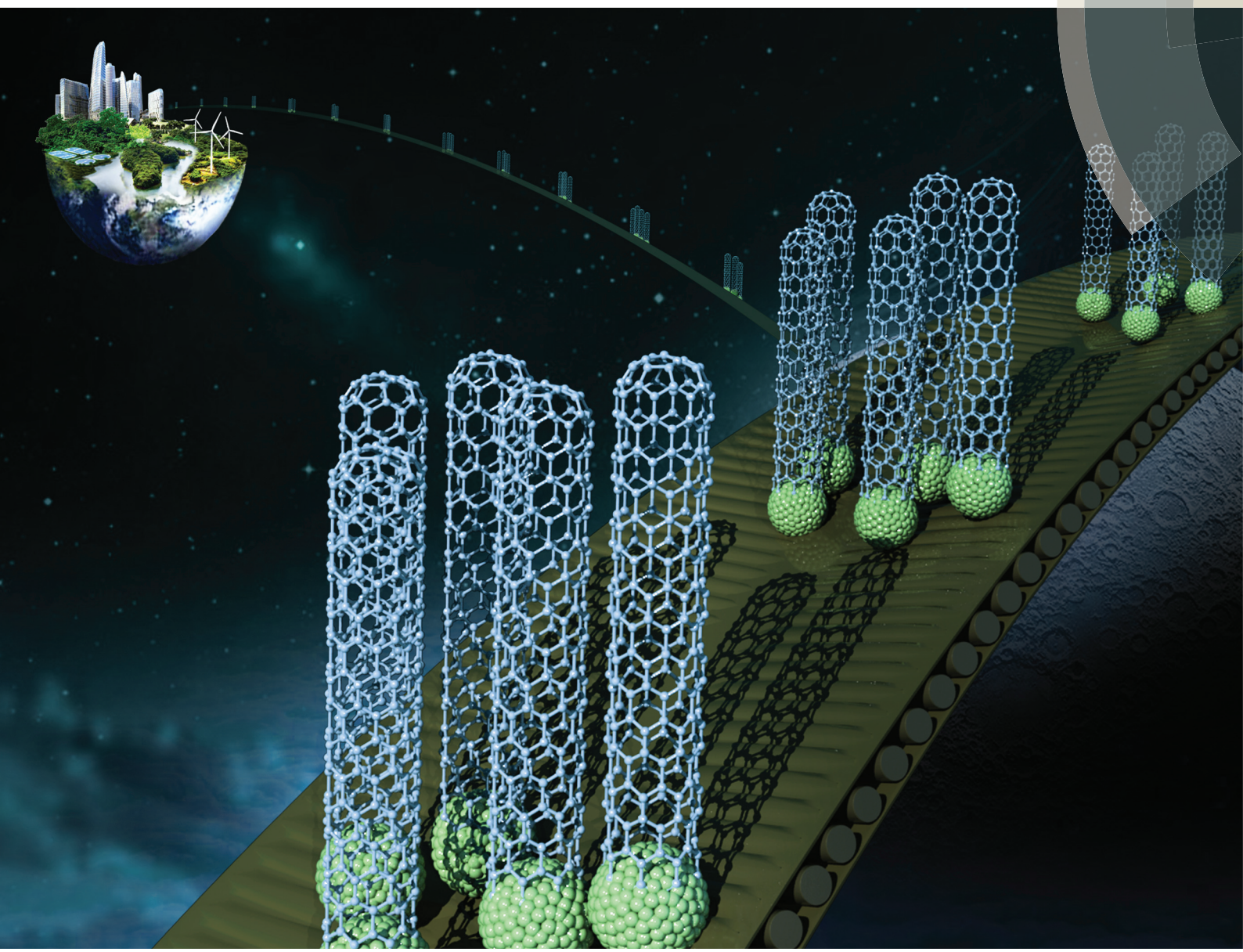

ISSN 1463-9262

ROYAL SOCIETY OF CHEMISTRY

CRITICAL REVIEW

Wenbo Shi and Desiree L. Plata

Vertically aligned carbon nanotubes: production and applications for environmental sustainability

Green Chemistry

CRITICAL REVIEW

View Article Online
View Journal | View Issue

Cite this: *Green Chem.*, 2018, **20**, 5245

Vertically aligned carbon nanotubes: production and applications for environmental sustainability

Wenbo Shi [a,b] and Desiree L. Plata *[a,b]

Received 15th July 2018,
Accepted 12th September 2018

DOI: 10.1039/c8gc02195c

rsc.li/greenchem

Carbon nanomaterials play an essential role in resolving the increasingly urgent energy and environmental crises. A unique type of carbon nanotubes (CNTs), vertically aligned CNTs (VACNTs) possess the intrinsic, extraordinary nanoscale properties (mechanical, electrical, and thermal) of individual CNTs, but present them in a hierarchical and anisotropic morphology, which holds promise to transform a diverse set of practical environmental application processes from water filtration to energy storage. Nevertheless, the potential environmental impacts beholden to their synthetic methodology might reduce the net sustainability benefits of this advanced material, where environmental impacts of the synthesis may be reduced or offset by the lifetime benefits of the proposed technologies. Aiming to provide a holistic view of the robust development of VACNT-enabled environmental technologies, this critical review assesses recent advances in their production routes and applications, both with a focus on environmental objective optimization. In particular, sustainable production of VACNTs, VACNT-based functional composite materials, and their environmental engineering applications based on different functional mechanisms (*i.e.*, sorption, catalysis, and separation) are thoroughly featured. Finally, we illustrate VACNTs as an example to explore strategies to co-optimize their environmental benefits and costs, which could potentially impact the way all other emerging materials are designed for environmental sustainability purposes.

1. Introduction

Their intrinsic chemical and mechanical properties, such as exceptional thermal and electrical conductivities, have inspired widespread research efforts on carbon nanotubes (CNTs).[1] Along with a boom in CNT-related publications and patents, CNT production has become a large-scale industrial chemical process, with annual production reaching a level of thousands of tons in the year 2011.[2] The favored method for CNT mass production is catalytic chemical vapor deposition (CVD),[3] which is a heterogeneous catalytic conversion process where carbon-containing gas species are converted to nanotubular graphitic structures with the assistance of nanoparticles under thermal treatment (note that CNTs can also be synthesized by arc discharge and laser ablation). Generally, as-grown CNTs display three different morphologies achieved *via* variable growth techniques: (1) agglomerated "powdered" CNTs, (2) horizontally aligned CNTs, and (3) vertically aligned CNTs (Fig. 1).

Agglomerated CNT powders are grown from fluidized bed reactors to take advantage of the uniform gas diffusion and heat transfer to metal catalyst nanoparticles in the CVD process. This production method is the easiest to scale, but inevitably causes mixing with impurities (amorphous carbon and catalyst), resulting in the need for post-synthesis treatment to yield pure CNTs. Impurities are removed by acid treatment/thermal annealing, which can introduce other structural impurities, degrade nanotube length and perfection, and inevitably add production cost and indirect costs associated with environmental damages. This form of CNTs is the most widely produced CNT today, dominating the annual production, whereas the contribution of aligned forms is trivial, and the powered CNTs have already been incorporated into commercial applications (*e.g.*, in bulk composite materials and thin films). In addition, high single-chirality abundance SWCNT powders are available after tedious post-synthesis selection processes or, for 6,5 (*n*,*m*) tubes, by careful catalyst selection used in a few commercial products.[7,8] However, these unorganized CNT architectures usually fail to meet expected material properties, likely due to poor alignment, loss of anisotropy, or loss of nano-dependent features through the formation of an agglomerated structure. For example, others have shown that whereas isolated CNTs were highly thermally conductive, their unorganized assemblies behaved more like thermal insulators due to the contact resistance of CNT overlaps or junctions.[9] The production and applications of agglomerated CNTs have been reviewed previously.[10–16]

[a]*Department of Chemical and Environmental Engineering, Yale University, New Haven, Connecticut, 06511, USA*
[b]*Department of Civil and Environmental Engineering, Massachusetts Institute of Technology, Cambridge, Massachusetts, 02139, USA. E-mail: dplata@mit.edu*

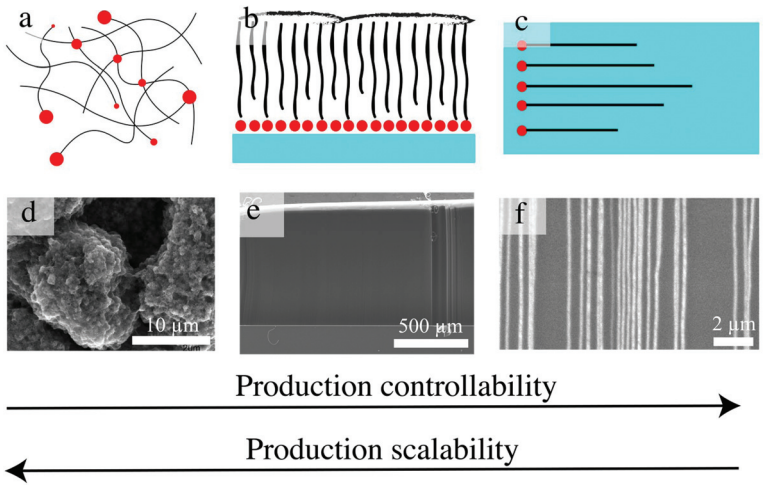

Fig. 1 Illustration of three as-grown CNT morphologies: (a) agglomerated CNTs, (b) vertically aligned CNTs, and (c) horizontally aligned CNTs through CVD and their corresponding SEM images (d–f). (d–f are reproduced from ref. 4 with permission from Elsevier, ref. 5 with permission from the Royal Society of Chemistry, and ref. 6 with permission from Copyright 2014 American Chemistry Society, respectively.)

In contrast to powdered, agglomerated products, horizontally aligned CNTs and VACNTs provide flat and/or substrate-bounded growth, which directs them into organized morphologies. Horizontally aligned CNTs have the highest crystallinities, but suffer extremely low yields (areal density usually less than 200 CNTs μm^{-1} (ref. 17)). In addition, they have narrow and confining, although potentially transformative, application fields, specifically for nanoscale electronic devices. However, a lack of chirality control, low number density, and precise placement are current challenges faced by the scaled development of this CNT form. The advances in the controlled synthesis of horizontally aligned carbon nanotubes and their applications were reviewed recently.[18–24] Here, we note that a "trick" to achieve horizontally aligned tubes requires a relatively low areal density of deposited catalyst (*i.e.*, catalyst deposited in a 1D line that gives rise to orthogonal tube growth) and strong tube–substrate adhesion. In contrast, a high areal density of the catalyst provided with an appropriate C feeding rate (high enough to sustain the nucleation and elongation of high density tubes simultaneously) can promote the formation of vertically aligned, substrate-bound CNTs. This anisotropic and 3D macroporous morphology renders the unique properties of a fully accessible surface area, little-to-no amorphous carbon, minimal residual catalyst, 1D ballistic mass transport

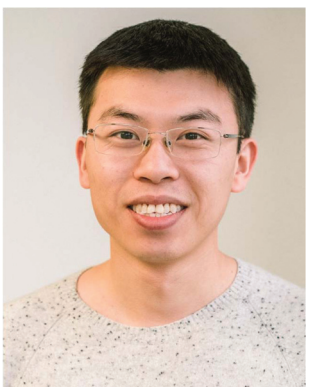

Wenbo Shi

Wenbo Shi is a Postdoctoral Associate in the Department of Civil and Environmental Engineering at MIT. Before joining MIT, he received a B.E. in Environmental Engineering from Tsinghua University (Beijing, China), a M.S. in Civil and Environmental Engineering from Duke University, and a Ph.D. in Chemical and Environmental Engineering from Yale University. He is interested in the sustainable production of advanced nanomaterials and is dedicated to promoting their application in energy and environment-related fields.

Desiree L. Plata

Desiree Plata's research seeks to maximize technology's benefits to society while minimizing environmental impacts of industrially important practices through the use of geochemical tools and chemical mechanistic insights. Plata earned her doctoral degree in Chemical Oceanography and Environmental Chemistry from the MIT/Woods Hole Oceanographic Institution's Joint Program in Oceanography and her bachelor's degree in Chemistry from Union College in Schenectady, NY. Plata is a National Academy of Engineers Frontiers of Engineering Fellow, a two-time National Academy of Sciences Kavli Frontiers of Science Fellow, and an NSF CAREER Awardee. Plata is currently Gilbert W. Winslow Career Development Assistant Professor of Civil and Environmental Engineering at the Massachusetts Institute of Technology.

through tube pores,[25] high electrical conductivity, and mechanical, chemical, and electrochemical stability, which lead to their broad proposed application in supercapacitors,[26,27] electronic interconnects,[28] emitters,[29] dry adhesives,[30] mechanical materials,[31,32] separation membranes,[33,34] advanced yarns and fabrics,[35] black-body absorption,[36] high-resolution printing stamps,[37] optical rectennas,[38] chemically driven thermopower wave guides,[39] and ultrasensitive virus detection.[40] Among these applications, the environment- and energy-related ones are in urgent need of development (*i.e.*, for implementation to tackle the environmental and energy crises). Due to the critical role of advanced materials in solving environmental and energy problems, these applications were reviewed recently for other emerging hierarchical nanomaterials (*e.g.*, graphene-based nanomaterials,[41–45] transition-metal dichalcogenide nanomaterials,[46,47] and metal–organic frameworks[48]), but VACNTs, although exceptional among CNT forms, have not been summarized or forecast. This review aims to provide a holistic analysis of the robust development of environmental optimization objectives for related VACNT production, architecture fabrication, and potential applications. Specifically, this review lays out routes to sustainable synthesis of VACNTs with minimized energy and emission burdens, and goes on to describe how these VACNT hierarchies might transform environmental materials applications. The ultimate goal is to employ advanced materials to achieve environmental and economic sustainability by working at the interface of material and environmental engineering.

2. Environmentally optimized synthesis

Incorporating environmentally-motivated perspectives into chemistry, engineering, and process design is essential to maximize benefits and minimize the risks of novel material and technology design.[49] Engineered nanomaterial (ENM) synthesis enables potentially transformative nanotechnologies, which allow humans to access previously unattained material properties. Nevertheless, the chemical process associated with ENM production might exert adverse impacts on the environment and human health. Regarding CNTs, and particularly those with controlled 3D morphologies, the intensive energy and resource consumption of current synthetic routes raises environmental concerns for future industrialization.[50–52] That is, early synthetic interests focus on controllability to achieve the desired device performances with little focus on environmental impacts, and because early design choices often propagate to the scaled processes, early omissions of impact prevention can lead to catastrophic damages for industry (*e.g.*, asbestos,[53] bisphenol A,[54] or methyl-*tert*-butyl ether[55]).

Similar to other industrial processes, environmental impact investigations of CNT production are delayed by roughly 20 years from the onset of the invention.[5] In 2008, Healy *et al.*[50] conducted the first life cycle assessment (LCA) on CNT manufacturing *via* arc ablation, CVD, and high-pressure carbon monoxide, and they highlighted that the life cycle impacts were dominated by energy consumption. Indeed, CNTs were found to be among the short list of the most energy-intensive materials syntheses, of the order of up to 100 times more than aluminum.[51] In addition to the specific energy requirements, toxic byproduct emissions from CNT production might exert potential human health impacts,[56] where environmental impacts from emissions can exceed direct exposure impacts.[57] Aware of the potential environmental concerns of CNT production, more studies on environmental optimization of CNT manufacturing were inspired by these pioneering works, and several milestones have been achieved (Fig. 2).

Atomic carbon conversion efficiency and thermodynamic limitations are the fundamental chemical drivers that directly control byproduct generation and minimum energy cost, respectively. The atomic carbon conversion efficiency for agglomerated, bulk powdered CNTs is almost universally higher than that for vertically aligned CNTs due to the contact

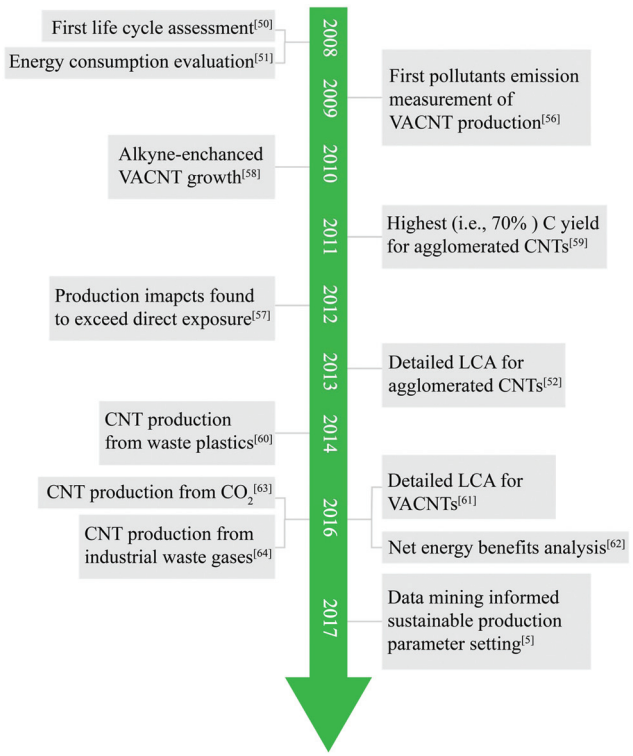

Fig. 2 Timeline of milestones of CNT production studies pertaining to environmental optimization objectives. These efforts include the following discoveries: the first life cycle assessment (LCA) of CNT production,[50] energy consumption evaluation,[51] the first pollutant emission measurement for VACNTs,[56] alkyne-enhanced VACNT growth,[58] the highest reported carbon conversion efficiency for agglomerated CNTs,[59] production impacts found to exceed direct exposure impacts for CNTs,[57] detailed LCA for agglomerated CNTs,[52] CNT production from waste plastics,[60] detailed LCA for VACNTs,[61] net energy benefit analysis for CNT applications,[62] CNT production from CO_2,[63] CNT production from industrial waste gases,[64] and the first data mining for CNT growth recipes and improved efficiency strategies.[5]

between the reactant gas and more available catalytic sites (*i.e.*, large amounts of catalyst are loaded and mixed in contact with the reactant C source). For example, Kim *et al.*[59] developed a semi-continuous fluidized-bed with augmented catalyst dispersing on ceramic beads, reaching a remarkable atom efficiency of over 70%; in contrast, the VACNT grown from substrate-affixed catalysts and C_2H_4-fed chemistry exhibited only 0.05%[5] C conversion. Note that the residual input gaseous materials are all exhausted as environmental pollutants (*i.e.*, volatile organic compounds (VOCs) and polycyclic aromatic hydrocarbons (PAHs)), and thus low yields necessarily correspond to high emissions rates (unless recycling is used, which is rare[65–68]). Low carbon conversion efficiency is influenced by reactant imbalances and poor contact, but could be exacerbated by some thermodynamic limitations. Thermodynamic insights are popular to explain the resulting CNT controllability; for example, SWCNT selectivity commonly relies on minimized formation energy to determine the geometrical association between CNT structure and one specific crystal lattice of the catalyst during active carbon species arrangement.[21] However, from the overall energy consumption perspective, the conversion from the starting carbon materials to the active carbon species tends to correlate with the minimum operational temperature requirements, which are related to energy costs.[5] In fact, most previous successful approaches for lower temperature CNT synthesis reflected the elimination of this carbon precursor conversion process, including plasma enhancement,[69,70] preheater implementation,[71] and more active gas precursor choice.[72]

To achieve better yield, the CNT growth *via* CVD has been modified through advancing reactor design and altering chemical processes. Simultaneously, these approaches happen to benefit the environmental sustainability of CNT manufacturing. Two successful representative reactor design modifications include controlling the gas flow direction (*i.e.*, employing a gas shower system to deliver gas from the top of the forest instead of from the side)[73] and manufacturing CNTs in a continuous manner,[74] both of which serve to maximize the contact between the gaseous reactants and catalyst and enhance the yield performance. While reactor setup modification is a promising strategy, it is often less accessible once significant capital costs have been invested, and manipulating the chemical reaction process is a more common strategy to enhance the carbon yield, including investing in heteroatom growth enhancers (*e.g.*, H_2O,[75–80] O_2,[78,81–84] H_2,[59,85] alcohol,[86,87] CO_2,[72,88,89] and acetone[90]) or/and altering the hydrocarbon source.[58] In addition, new branches of research aimed at using waste streams for CNT production have gained attention recently, including CNTs from waste plastics,[60] converting CO_2 to CNTs,[63,91] and utilizing industrial gas effluents as CNT feedstock material,[64,92] which hold promise to enhance the environmental sustainability due to reaction source accessibility and low cost.

Based on the CVD process of CNT synthesis, a strategic modification route (Fig. 3) to promote sustainable production of CNTs is proposed. From changing the starting materials to increasing the catalyst efficiency, to reusing effluent gases, each modification (either through chemistry or reactor design) would advance the economic and environmental sustainability of this energy and material-intensive process. The synthetic strategy not only determines the overall sustainability of the production–application circuit, but also is critical to tune as-grown CNT properties for desired applications (*e.g.*, alignment for shorted charge or thermal transport path and diameter for filtration).

3. Integration in VACNT-composite functional materials

In addition to the manipulation of VACNT growth, chemical and structural modifications are commonly employed to preserve the structural stiffness or to introduce new functionalities into the hierarchical porous platform of VACNTs. VACNT–polymer composites,[93] VACNT–inorganic hybrids,[94] and heteroatom doped VACNTs[95] are important derivatives to serve as functional materials for environmental and energy beneficial purposes (Fig. 4). Since VACNTs will experience surface-tension driven aggregation and densification following liquid infiltration and evaporation,[96] the traditional treatment methods (*e.g.*, mechanical-reinforced solution dispersion or strong acid oxidation) used with powdered CNTs can not be used with VACNTs in order to form these VACNT-composites if

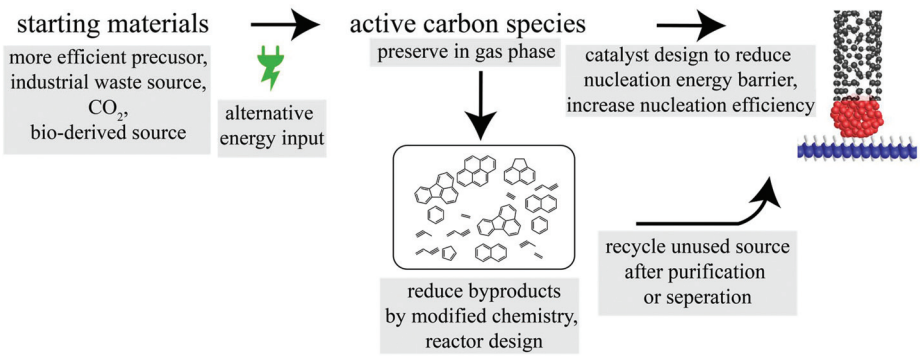

Fig. 3 Flow chart of CNT synthesis steps and modification suggestions (grey boxes) for future environmentally sustainable CNT production.

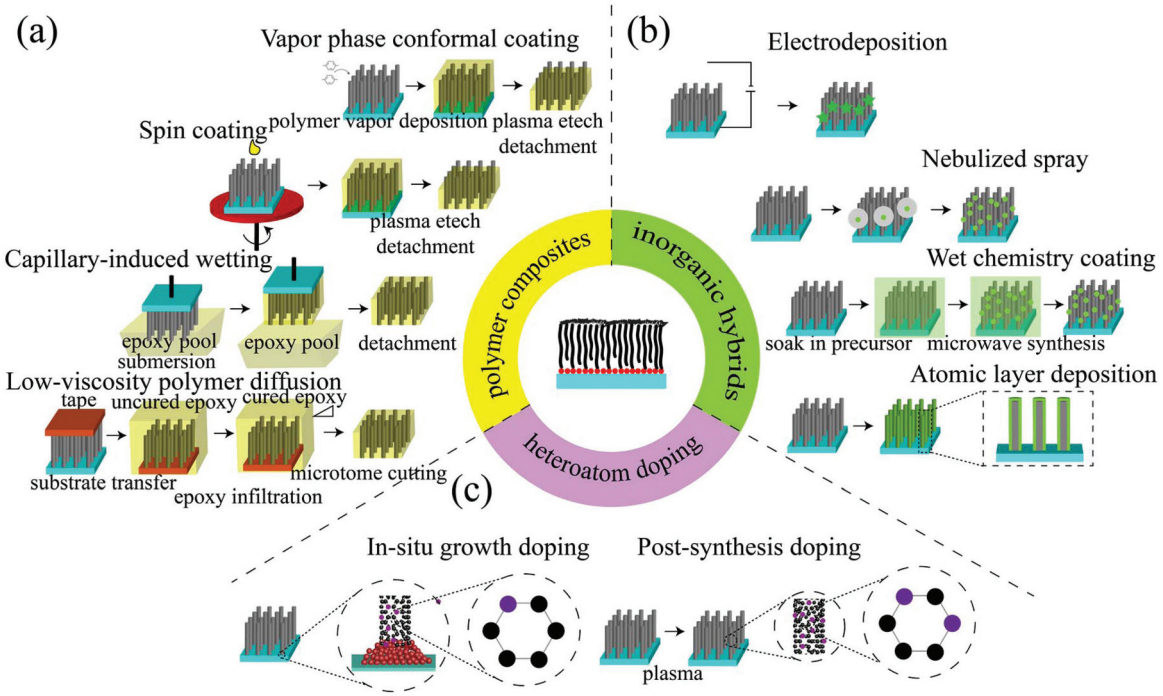

Fig. 4 Schematic illustration of VACNT-enabled functional materials and their corresponding fabrication methodologies. (a) VACNT–polymer composites, (b) VACNT–inorganic hybrids, and (c) heteroatom-doping VACNTs. Note that the heteroatom (purple) in c is merely a schematic illustration of the concept and the newly-formed structure doesn't necessarily still retain a hexagonal structure after heteroatom doping.

one seeks to preserve their 3D structure. With this constraint, a wide array of unique fabrication methods have been developed to achieve VACNT-composite functional materials, which confer VACNTs new properties (*i.e.*, catalysis) or augment the properties of individual components for superior overall performance.

For demanding applications requiring optimized permeability and selectivity, such as wastewater treatment membranes, open and aligned nanochannels of VACNTs are the unique characteristic needed to achieve fast mass transport through these superhydrophobic nanochannels.[25,33] Polymer infiltration would maintain the integrity of the VACNTs under their functioning environment (*e.g.*, pressurized or aqueous conditions) and guarantee that the targeted molecule(s) travel through the defined nanopores only. Such VACNT–polymer composites have been efficiently fabricated through vapor phase conformal coating polymers,[34,97] spin coating polymers,[33,98] capillary-induced wetting polymer infiltration,[31] and direct polymer diffusion through immersing VACNTs in a polymer solution[99,100] (Fig. 4a). Spin coating, capillary-induced wetting polymer infiltration, and direct polymer diffusion are easy to operate and are sufficient to accomplish the target of blocking the interstitial space between tubes in the VACNT forest. In contrast to these solution-based polymerization techniques, vapor phase polymer coating methods utilize the polymerization of delivered vapor-phase monomers on the surface of the substrate, which could result in more controllability.[101] The tunable, conformal coating not only is capable of forming a VACNT membrane, but also might enable additive functionalities (*e.g.*, superhydrophobicity[102]) onto VACNTs.

In the VACNT–inorganic hybrids, VACNTs work as a support in most cases to maximize the performance of active inorganic components, usually by functionally increasing their exposed surface area, such as for catalysis and/or adsorption. Compared with other large surface area supporting materials, the unique advantages of VACNT are their synergistic characteristics of high conductivity and well-ordered hierarchical structures. The metal oxides or metals can be deposited through electrodeposition,[103] nebulized spray,[104] wet chemistry coating,[105,106] and atomic layer deposition[107,108] (Fig. 4b). Electrodeposition and wet chemistry methods are solution-based coating approaches. Due to the capillary-driven aggregation of the CNT forest upon liquid infiltration and evaporation,[96] these two techniques usually result in large coating particle size or non-uniform coating. Atomic layer deposition utilized a sequential self-terminating reaction between the gas phase molecules and the solid surface to ensure the extreme coating controllability (less than one nanometer),[109] but this process needs to operate in a special apparatus. To avoid liquid contact and overcome the difficulty of limited device accessibility, an interesting nebulized spray method was developed in 2014 and was found to work universally for different metal oxides.[104] Besides the VACNT–metal oxides, VACNT–graphene hybrid materials[110,111] have emerged as a promising

composite for energy storage devices due to the efficient covalent bonding between these two types of materials when forming 3D architectures, and they are usually made by CVD to deposit graphene and VACNTs on the substrate consecutively.

In contrast to coating metal oxides on the outer surface of VACNTs to serve as the catalytic active sites, replacing carbon atoms in the VACNT structures with heteroatoms (*e.g.*, N, S, B, and P) could directly introduce active sites inside VACNTs, rendering them highly efficient, metal-free catalysts.[112] These dopants can change the physical and chemical properties of VACNTs through inducing CNT graphitic structure charge redistribution and lattice structure distortion, leading the VACNTs to convey catalytic activity.[113] The heteroatom doping can be realized through *in situ* doping during VACNT synthesis[114–116] or doping during post-treatment[117] (Fig. 4c). *In situ* doping processes are conducted *via* co-delivering the C-containing precursor and the heteroatom-containing precursor for the catalytic thermal CVD process, whereas post-treatment doping relies on incorporating heteroatoms into the existing vacancies in the graphitic lattice. This results in the traditional post-synthesis thermal annealing that is not compatible with well-crystalline SWCNTs (*i.e.*, nearly no N- or S-doping is available)[118] and the highest N doping level (5.0 at%, defined as mol heteroatom/mol C × at%) was achieved through *in situ* synthesis.[119] Considering plasma etching has been used to open VACNT caps as well as functionalize them, that technique, simultaneously generating graphitic vacancies and incorporating heteroatoms into these sites, might emerge as an alternative post-synthesis treatment approach to doping VACNTs under a N_2 or NH_3 gas environment.[120–122]

4. Environmental applications of VACNTs

While there are a large number of environmental applications proposed for CNTs, three categories have garnered the most attention, leading to the most notable demonstrations. These are in the areas of sorption, catalysis, and separations (*via* size sieving) (Fig. 5).

4.1 Adsorption

Adsorption processes are a traditional technique in point-of-use devices to selectively remove viruses, inorganic and organic pollutants to produce clean and safe water or gas.[123] Due to their high surface area, well-defined pore structures, inherent hydrophobicity, and tunable nanoscale properties, CNTs have been considered as remarkable adsorption materials in the past few decades. Although most studies utilized randomly oriented CNTs, previous efforts have identified four possible adsorption sites in CNT bundles:[11,124] (1) the hollow interior of individual nanotubes, (2) the interstitial channels between individual nanotubes inside nanotube bundles, (3) the external groove site where two outermost adjacent parallel tubes meet, and (4) the curved surface of the outermost, "exposed" nanotubes at the edges of the nanotube bundles (Fig. 6a). Note that functional groups and defects in the CNT structure may change the accessibility and affinity of CNT surfaces for sorbates, dramatically altering the adsorption behavior.[125] Interestingly, alignment has emerged as a critical factor to control adsorption capacity, ultimately allowing free-standing VACNT films to fulfill their promise to outperform randomly oriented CNTs. For example, using N_2 adsorption as the study model, the self-oriented CNT vertical arrays were found to deliver increased adsorption uptake compared to the disarranged counterparts following ultrasonication treatment, due to the enhanced interstitial spaces between the individual nanotubes inside the VACNTs, along with better alignment.[126] The potential adsorption applications of VACNTs for environmental remediation and energy engineering are categorized in the following discussion into (1) gas phase adsorption, (2) liquid phase adsorption, and (3) ion adsorption from liquid systems (Fig. 6).

4.1.1 Gas phase adsorption. Adsorption technologies have played a vital role in gaseous pollutant management due to their fast reaction kinetics, simple design and operation, and sometimes low cost. CNTs have been investigated as adsorbents for removing key pollutants (*e.g.*, NO_x,[127] SO_2,[128] VOCs,[129–131] and CO_2[132–134]) that either are toxic to human health, hazardous to environmental ecosystems, or contribute to climate change from waste gas streams. However, available examples using VACNTs as gaseous pollutant adsorbents are extremely limited. Babu *et al.*[135] studied double-walled VACNT

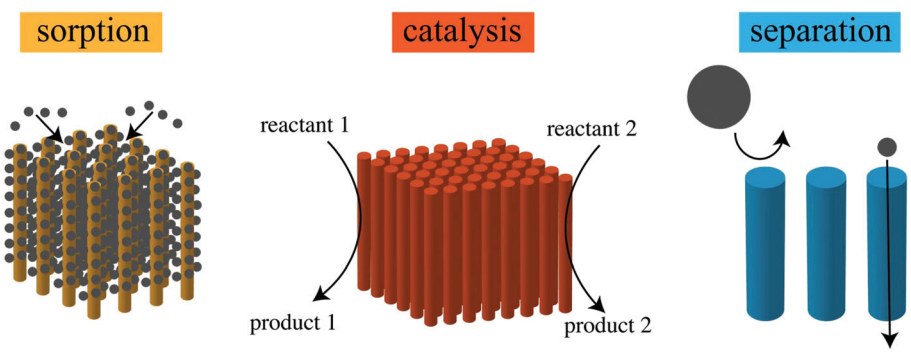

Fig. 5 Schematic illustration of the environmental applications of CNTs, including sorption, catalysis, and separation.

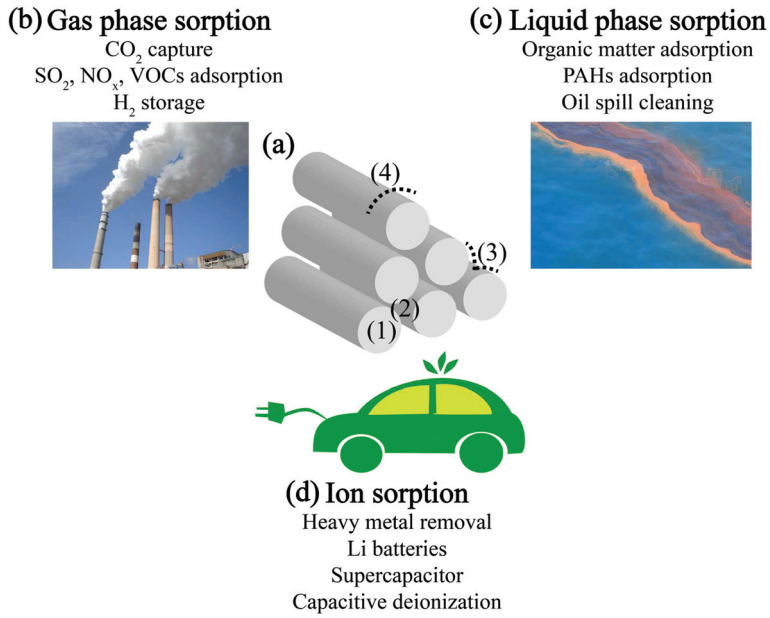

Fig. 6 (a) CNT bundles' possible adsorption sites and (b–d) CNTs' adsorption functional mechanisms for environmental and energy engineering purposes at different media–CNT interfaces.

forests with varied average diameters and discovered that decreasing the CNT diameter could increase the adsorption capacity of CO_2 at high pressure regimes (ranging from 5 to 60 bar). To potentially enhance the adsorption performance at low pressure (less than 15 bar), the authors found that oxygen plasma could functionalize the VACNTs with C–O functional groups *in situ* without impacting the well-ordered 3D structure, and the product exhibited better adsorption characteristics. Here, we note that most VACNT adsorption studies still remain in the theoretical prediction stage,[136–141] but all indicate the superiority of this unique morphology as effective adsorbents, merely due to their well-defined open-end pore arrangement and tunable inter-tube space when compared to their powdered CNT counterparts.

In addition to the gas pollutant remediation-oriented gas phase adsorption, the signature adsorption characteristic enables CNTs to store H_2 [142,143] for energy generation, providing a critical solution to "renewable" energy storage and transformation. When using VACNTs, Cao *et al.*[144] demonstrated that controlling the inter-nanotube space between adjacent parallel tubes could contribute more H_2 storage capacity enhancement space as the supplement to the generally suggested hollow interior storing space of individual nanotubes. However, over the evolution of this technique, there has been substantial controversy regarding the reported H_2 uptake capability of CNTs,[145] and this hinders advancement of this technology. Poignantly, this highlights the importance of reproducibility while developing applications for advanced materials and the threshold for rigor that should be applied for robust proof-of-concept demonstrations.

4.1.2 Liquid phase adsorption. Many hydrophobic sorbents are used to enhance partitioning of dissolved organic chemicals (*i.e.*, the sorbates) from the aqueous phase to the solid sorbent, and while VACNTs are effective in this mechanism of uptake, their unique geometry can offer wicking and sponge behaviors that enhance chemical partitioning *via* physical uptake. Accordingly, a representative proposed application of 3D CNT structures in liquid phase adsorption is oil spill cleaning. Using a similar growth methodology to produce VACNTs (*i.e.*, CVD) but with a different carbon source (*i.e.*, ferrocene dissolved in 1,2-dichlorobenzene as a catalyst precursor and a carbon source, respectively, fed by a syringe pump), a CNT sponge with a porous, interconnected, and 3D framework was fabricated and it exhibited an exceptional (*i.e.*, up to 180 times its own weight, about 100 times higher than activated carbon) oil adsorption capacity.[146] In addition to those physical drivers for sorption, chemical modification was shown to improve sorption capacity; for example, boron substitution doping created covalent bonding between the 3D, interconnected CNT skeleton, which enhanced the oil adsorption performance and enabled sorbent reuse.[147] In addition to oil uptake, aromatic compounds (*e.g.*, dioxin,[130] benzene,[125,148] phenol,[149] and PAHs[150]), humic acid,[151] and dye molecules[152] can also be adsorbed by CNTs. However, similar to gas phase adsorption studies, these explorations are limited to randomly-oriented and aqueous-solution-dispersed CNTs derived from powdered CNTs.[125] Nevertheless, the sorptive properties of these powdered CNTs are as good or better on both a mass and surface-area normalized basis than granular activated carbon sorbents.[153,154] Compared to powdered CNTs and activated carbons, where most of the carbon mass is internal and inaccessible to large sorbates, VACNTs have theoretically maximized surface areas, tunable functional groups, great accessibility to the adsorbates, intrinsic chemical stability, and, most importantly, their bulk structure integrity could result in

orders of magnitude adsorption enhancement and reuse properties that are beneficial for real world applications.

4.1.3 Ion sorption. Ion sorption is the fundamental property that enables heavy metal removal, electrochemical desalination, supercapacitors, and batteries; that is, most of the energy storage applications rely on this property of CNTs. The nanoporous structure, enormous number of available adsorption sites, and high conductivity enable CNTs to act as the active component in devices for both water treatment and energy storage, potentially tackling the water scarcity and energy crises (and some have proposed that this could be done simultaneously[155,156]). The available heavy metal ion adsorption investigations are mostly confined to randomly oriented and solution-dispersed CNTs, and several studies have claimed that surface functional group density is the key control factor to enhance heavy metal adsorption capacity.[157–162] In contrast, for energy storage applications, better control of ion and electron flow is required, and thus, VACNTs have been intensively explored for supercapacitors[26,27,163] and Li-ion batteries.[164,165] The 3D, well-ordered framework of these materials creates a more accessible surface area (*i.e.*, confers mesoporosity[166]) and well-directed electron transport paths for electrochemical ion adsorption. While maintaining a vertically aligned shape, densification[26,163] and nanotube cap opening[27] were found to enhance their capacitance as an electrical double layer capacitor, due to increased volumetric specific electrode surface area and accessibility of the inner cavity, respectively. Moreover, the VACNT surface could serve as a platform for metal oxide deposition, providing novel routes to CNT/metal oxides[103–106,167–170] materials that may perform as a hybrid capacitor/battery, which store charge relying on the electrochemical double layer (*i.e.*, electrostatically) and also *via* the fast surface redox reactions of metal oxides (*i.e.*, electrochemically). This additive electrochemical pseudocapacitance could augment overall total capacitance and contribute to the overall performance of the energy storage materials.

4.2 Catalysis

A perfect CNT structure does not exhibit outstanding catalytic capability. The catalytic activity relies on functional groups, defects, dopants, and decorated catalytic active species, where the catalytic activity can be enhanced by the presence of the CNTs. CNT-based catalysts provide high activity and durability because of their high surface area, high crystallinity, controllable homogeneity, chemically uniform active sites and stable geometric structure.[113,171,172] However, the majority of CNT-based catalysts have been explored for electrochemical fields, whereas non-electrochemical catalysis targeting industrially important transformation technologies (*e.g.*, environmental remediation) are still under development. Similar to the benefits of morphology (enhanced surface area) in adsorption, VACNTs have also shown improved catalytic performance with their corresponding functional composites (Table 1).

4.2.1 Catalysis in the liquid phase. Catalytic technology for liquid waste treatment includes catalytic ozonation, photocatalysis, electrocatalysis, and electron-Fenton systems, which could efficiently remove organic compounds (*e.g.*, pesticides, pharmaceuticals, and personal care products), nitrates, and other aqueous pollutants.[183] Even though CNTs were reported to benefit these processes,[184,185] they have been rarely used in a 3D form, except during photocatalysis. A good example of VACNTs' photocatalytic applications is to support and tune the properties of titanium dioxide, which is a widely used photocatalyst, but one that suffers from a low surface area and a

Table 1 Summary of VACNT-based catalysts and their catalytic processes for environmental and energy applications

Catalysis type	Functional materials	Catalytic reaction	Environmental and energy implications	Ref.
Photocatalysis	VACNT/TiO_2	*E. coli* bacteria inactivation	Water disinfection with solar energy	Akhavan *et al.*[173]
	VACNT/TiO_2	$2H_2O \rightarrow O_2 + 4H^+ + 4e^-$	Solar energy conversion	Yang *et al.*[174]
	CdS–CNT sponge	Rhodamine B dye degradation	Water purification	Li *et al.*[175]
	N-Doped CNT/TiO_2 core/shell nanowires	Methylene blue and *p*-nitrophenol dye degradation	Water purification	Lee *et al.*[176]
	TiO_2/CNT/Pt nanoarrays	Dye degradation: $2H_2O \rightarrow O_2 + 4H^+ + 4e^-$	Water purification and solar energy conversion	Park *et al.*[177]
Biocatalysis	VACNTs	Organic matter consumption by microorganism	Wastewater remediation and power generation	Mink *et al.*[178]
Electrocatalysis	Pt–VACNT–carbon fibers	$O_2 + 4H^+ + 4e^- \rightarrow 2H_2O$	Environmental sensor	Xiang *et al.*[179]
	VA–N-doped CNTs	$O_2 + 4H^+ + 4e^- \rightarrow 2H_2O$	Fuel cells; renewable and clean energy technology	Gong *et al.*[114]
Electrocatalysis	VA–N-doped CNTs	$CO_2 + 2H^+ + 2e^- \rightarrow CO + H_2O$	CO_2 reduction, climate change mitigation	Sharma *et al.*[116]
	VA–boron–carbon–nitrogen NTs	$O_2 + 4H^+ + 4e^- \rightarrow 2H_2O$	Fuel cells; renewable and clean energy technology	Wang *et al.*[180]
	VACNT/metal oxides	$O_2 + 4H^+ + 4e^- \rightarrow 2H_2O$	Fuel cells; renewable and clean energy technology	Yang *et al.*[104]
	MoS_x-VANCNTs	$2H^+ + 2e^- \rightarrow H_2$	H_2 production, renewable energy	Li *et al.*[181]
	Pt-VACNT	$CH_3OH + H_2O \rightarrow 6H^+ + 6e^- + CO_2$	Methanol oxidation, fuel cells, renewable and clean energy	Su *et al.*[182]

large band gap energy.[174,176,177] In addition to pollutant remediation and water splitting, a composite CNT-TiO_2 3D photocatalyst was found to photoinactivate bacteria under visible light irradiation (differing from the UV light irradiation of TiO_2 itself).[173] To achieve the same purpose of water disinfection, replacing TiO_2 with Ag in the VACNT arrays has been demonstrated to show strong antibacterial activity in the dark (no light required).[186]

4.2.2 Catalysis in the gas phase. Environmental catalysis also plays an essential role in gaseous pollutant control from both stationary and mobile sources with applications ranging from selective catalytic reduction of NO_x with NH_3, CO oxidation, Hg^0 oxidation, to VOC catalytic combustion.[187] The mode of participation in these reactions for CNTs is usually as the support or confinement for the active compounds.[188–193] Taking manganese oxide as an example (a highly efficient heterogeneous catalyst for gaseous pollutant removal[194]), employing CNTs as the support efficiently enlarges its surface area and thus enhances the catalytic performance.[195] Following the rising attention on the importance of the hierarchical geometric structure of the metal oxide catalysts,[196] VACNTs with well-defined nanoscale and macroscale structures could provide an outstanding platform to support and sufficiently disperse the active catalyst, paving the way for improved catalytic performance.

4.2.3 Electrochemical catalysis. A large portion of catalysis work using VACNTs is in the field of electrochemical catalysis, which is critical for renewable and clean energy technologies. These catalytic reactions include oxygen reduction,[104,114,180] hydrogen evolution reaction,[181,197] and CO_2 reduction.[116] VACNTs have demonstrated success when doped by heteroatoms (*e.g.*, nitrogen or boron) or decorated with metal/metal oxides, where CNT electronic properties were tuned (*e.g.*, by locally charging due to the difference in electronegativity of C and the substitutional elements or extra catalytic active sites due to the introduced metal cation incorporating in the graphitized carbon structure or embedding on the carbon plane) but their geometric features were maintained (*i.e.*, shorter electron transport path and better electrolyte or reactant diffusion). In addition to these traditional electrochemical systems, VACNTs have also been used as anodes in a bio-electrochemical system (*i.e.*, microbial fuel cells[178,198]), which is a technique that has been suggested to integrate organic waste remediation and electricity generation in one system *via* the bio-catalytic activity of microorganisms for waste water treatment.

4.3 Separation

CNTs have been proposed as nanochannels for fundamental nanofluidic studies and membrane-based separation applications,[199,200] due to their tunable nanoscale properties, uniform hollow geometry, molecularly smooth inner surface, and exciting fluid transport rate (Table 2). The fast size exclusion selectivity feature of CNT-based membranes enables promising applications ranging from water purification,[201,202] water desalination,[203] gas purification and separation,[204] and drug delivery,[205] to breathable and protective textiles.[206] Since the permeate selectivity heavily relies on the homogeneity of nanopore size, the application of CNT-enabled separation devices requires strict requirements on the synthetic controllability of CNT manufacturing.

4.3.1 Ion exclusion. Ion exclusion is the primary principle for VACNTs to serve as filters for water purification.[203] The atomically smooth and hydrophobic inner core of CNTs provides a high speed tunnel for water molecule transport (4–5 orders of magnitude flux enhancement),[207] while the diameter of the hollow cylinder serves as the gate keeper to exclude the undesirable permeates. Moreover, the functional chemistry on the tip of CNTs may enhance or tune the ionic selectivity, ultimately mimicking the rapid and selective ion transport in biological membranes.[208] Majumder *et al.*[209] first demonstrated the effects of CNT tip functionalization on the flux and selectivity of permeates, where grafting long chain functional molecules would decrease the pore size and adding anionically charge dye molecule onto the CNT core entrance would enhance the flux of cationic permeates (*i.e.*, methyl viologen MV^{2+} and ruthenium bipyridine $Ru(bipy)_3^{2+}$). Furthermore, Fornasiero *et al.*[210] proposed that the electrostatic interactions between the CNT membranes and mobile ions drove the ion rejection phenomenon, rather than steric or hydrodynamic effects when the narrow tubular confinement channel (CNT inner diameter) was larger than the diameter of hydrated ions. In addition, the capability of being able to independently functionalize each side of the VACNT membrane entrance[211] and the potential utilization of electrophoresis[212,213] could further stimulate membrane science with a viable route towards overcoming the tradeoff between permeability and selectivity.

4.3.2 Gas separation. Besides ion exclusion in liquid interfaces, VACNT membranes also function in gas interfaces. VACNT membranes for gas molecular separation could be used for natural gas dehydration,[214] H_2 production,[215,216] CO_2 removal,[217] air separation,[218] and membrane-distilled water desalination.[219] The transport of gases in CNTs was predicted to be over one order of magnitude faster than similar sized zeolites, which are commonly employed for selective gas separation at the expense of low flux.[220] The theoretical predictions have been verified by Hinds *et al.*[33] with multi-walled CNT (MWCNT) membranes (4.3 nm inner diameters) and Holt *et al.*[25] with double-walled CNT (DWCNT) membranes (sub-2 nm diameters) independently. CNT gas permeability selectivity has been demonstrated for hydrocarbon/He,[25] CO_2/CH_4,[221] H_2/CH_4,[216,222] H_2/CO_2 [216] mixtures, all of which have practical gas separation implications. It is noteworthy that the fast water vapor transport in carbon nanotubes has far-reaching implications, which could enable membranes for gas separations applications including, but not limited to breathable and protective fabrics, moisture control, and desalination *via* distillation.[206] Combining this ultrafast water transport property and VACNTs' strong optical absorption behavior enabled VACNTs to perform well in the solar–thermal–steam generation system (evaporation rate 10 times higher than bare water with a 90% solar thermal conversion efficiency),[223] providing a low cost, renewable energy-based desalination technique.

Table 2 VACNT-based nanofluid devices and their performed permeation tests

Interstitial filler	CNT diameter	CNT forest height (μm)	Area size (cm^2)	Fluid test	Ref.
Silicon nitride	20–50 nm	5–10	0.196	Water permeability	Holt *et al.*[224]
Silicon nitride	Average diameter 1.6 nm	2–3	4	2 nm gold particle and Ru^{2+} $(bipy)_3$ permeability; gas selectivity	Holt *et al.*[25]
Silicon nitride	Average diameter 1.6 nm		0.00175	Ion rejection of salt solution (K_3FeCN_6, KCl, pyrenetetrasulfonic acid tetrasodium (Na_4PTS), K_2SO_4, $CaSO_4$, $CaCl_2$, $Ru(bipy)_3Cl_2$)	Fornasiero *et al.*[210]
Polystyrene	30 ± 10 nm outer diameter, 4.3 ± 2.3 nm inner-core diameter	5–10	3.1	N_2 and $Ru(NH_3)_6^{3+}$ ionic species permeability	Hinds *et al.*[33]
Polystyrene	6.3 nm MWCNT diameter	10	3.1	Gas (He, H_2, and N_2) permeability	Mi *et al.*[98]
Polystyrene	7 nm pore diameter	126	0.3	Gas, liquid permeability, ions transport	Majumder *et al.*[225]
Urethane monomer	4.1 nm average pore size	1000	0.067	Polyethylene oxide rejection, water permeability	Lee *et al.*[226]
Parylene–N	3.3 nm average diameter	20–30	1.8	Charged dyes, 5 nm Au nanoparticle, 40–60 nm Dengue virus rejection; water vapor transport	Bui *et al.*[34]
Polysulfone	1.2 nm average pore diameter	0.6	13.8	Single gas permeability and mixed gas selectivity	Kim *et al.*[221]
Polystyrene–polybutadiene (PS–PB) copolymer	Average 3.3 nm diameter	20–50	cm^2 scale	5 nm gold nanoparticle, $K_3Fe(CN)_6$ and Direct Blue 71 permeability; gas permeability	Kim *et al.*[97]
Epoxy resin	8 nm average diameter	1000	1	None	Wardle *et al.*[31]
Epoxy resin	7–14 nm diameter	7000	4	Various liquid (water, ethanol, hexane, decane, *N*,*N*-dimethylformamide (DMF), dodecane, and 2-propanol) permeability	Du *et al.*[99]
Epoxy resin	4.8 nm diameter	200	0.1	Liquid permeability	Baek *et al.*[227]
None	2.8 nm inner tube	750	0.25	Gas permeability and selectivity; 3.2 nm gold nanoparticle permeability	Yu *et al.*[228]
None	6.7 inner diameter, 10 nm outer diameter	4000	0.25	Gas permeability and their selectivity *vs.* H_2O	Yoon *et al.*[214]
None	After densification, 7 nm outer wall pore	1300	1	Water permeability, dextran rejection	Lee *et al.*[100]

5. Conclusion and outlook

VACNT arrays with a hierarchical and anisotropic morphology effectively extend the intrinsic yet extraordinary nanoscale properties (mechanical, electrical, and thermal) of individual nanotubes to the macroscale, which hold promise to transform a diverse set of practical environmental application processes (sorption, catalysis, and separation) that will ultimately enable enhanced sustainability. The route towards realizing these goals requires sufficient integration of controllable, scalable, reproducible, and sustainable VACNT production, and effective functional composite fabrication (*i.e.*, tailored for targeting applications and functioning environments), and there have been some primary challenges limiting the broad adoption of these nano-enabled materials.

The challenges in controllability must be addressed through further efforts: the narrowest diameters produced so far (sub-1.5 nm (ref. 229)) in VACNT still do not meet the requirement for desalination (0.8 nm (ref. 230)), a further increase of the areal number density is necessary to enhance ion storage performance,[231] and bulk property homogeneity requires alignment control.[232] In addition to controllability challenges, production sustainability has emerged as an overlooked factor for future large-scale manufacturing, where proactive efforts are urgently needed. The relatively poor environmental performance associated with VACNT manufacturing is largely attributed to the limited fundamental understanding of the CNT growth process. Unveiling this is critical to eliminating unnecessary heating steps for reactive intermediate generation, which could reduce energy and resource costs.[58,233] In addition, the scaled-up manufacture of VACNTs is still rare, which gives rise to the gap between their bench scale application tests and practical industrial scale processes. Taking the VACNT-membrane as an example, most reported devices are in the cm^2 size range, whereas wafer-scale or m^2 scale membranes are necessary for real-world applications. Nevertheless, progress has been made in this area and routes toward such scaled synthesis are readily traceable.[74,234]

While essential concepts and methods for VACNT-enabled advanced materials have been proposed and demonstrated (*e.g.*, VACNT–inorganic hybrids, VACNT–polymer composites, and heteroatom-doped VACNTs), challenges such as lacking facile substrate transfer methods[235] and the undesirable structural deformation in functioning environments (*e.g.*, elastocapillary densification in aquatic environments[236]) are persistent challenges that remain in order to accomplish the goals of ultimately incorporating VACNTs into device configurations. The stable, robust, and safe device (*i.e.*, integrated system) design is closely related with not only the functional performance

durability, but also the prevention of potential nanomaterial release during device operation.

Another aspect of robustly developing VACNT-enabled environmental technologies is to integrate proactive environmental and economic analyses into the device design, use, and disposal for guiding their environmental and economic optimizations. LCA studies have been deployed for engineered nanomaterials and even CNT-based applications.[62,237–239] However, few of them have differentiated CNTs from their morphologically distinct counterparts; thus, studies focused on VACNTs and their enabled innovative technologies are limited.

Finally, this review aims to inspire the methodologies to holistically incorporate environment-driven perspectives into VACNTs: not only discussing their innovative application opportunities in environmental and energy engineering, but also featuring efforts to promote their production in a sustainable manner. This critical thinking and panoramic view based insight of co-optimizing environmental benefits and environmental costs should be expanded to the development of other emerging nanomaterials and could ultimately promote green nanotechnology to maximize the benefits for future environmental and economic sustainability.

Conflicts of interest

The authors declare no competing financial interests.

Acknowledgements

This work was supported by NSF Award Number 1552993, EPA grant number RD83558001, and Yale University graduate fellowships.

References

1 H. J. Dai, *Acc. Chem. Res.*, 2002, **35**, 1035–1044.
2 M. F. L. De Volder, S. H. Tawfick, R. H. Baughman and A. J. Hart, *Science*, 2013, **339**, 535–539.
3 G. D. Nessim, *Nanoscale*, 2010, **2**, 1306–1323.
4 F. Wei, Q. Zhang, W. Z. Qian, H. Yu, Y. Wang, G. H. Luo, G. H. Xu and D. Z. Wang, *Powder Technol.*, 2008, **183**, 10–20.
5 W. B. Shi, K. Xue, E. R. Meshot and D. L. Plata, *Green Chem.*, 2017, **19**, 3787–3800.
6 J. H. Li, K. H. Liu, S. B. Liang, W. W. Zhou, M. Pierce, F. Wang, L. M. Peng and J. Liu, *ACS Nano*, 2014, **8**, 554–562.
7 M. Zheng, A. Jagota, M. S. Strano, A. P. Santos, P. Barone, S. G. Chou, B. A. Diner, M. S. Dresselhaus, R. S. McLean, G. B. Onoa, G. G. Samsonidze, E. D. Semke, M. Usrey and D. J. Walls, *Science*, 2003, **302**, 1545–1548.
8 M. S. Arnold, A. A. Green, J. F. Hulvat, S. I. Stupp and M. C. Hersam, *Nat. Nanotechnol.*, 2006, **1**, 60–65.
9 R. S. Prasher, X. J. Hu, Y. Chalopin, N. Mingo, K. Lofgreen, S. Volz, F. Cleri and P. Keblinski, *Phys. Rev. Lett.*, 2009, **102**, 105901.
10 M. S. Mauter and M. Elimelech, *Environ. Sci. Technol.*, 2008, **42**, 5843–5859.
11 X. M. Ren, C. L. Chen, M. Nagatsu and X. K. Wang, *Chem. Eng. J.*, 2011, **170**, 395–410.
12 S. C. Smith and D. F. Rodrigues, *Carbon*, 2015, **91**, 122–143.
13 C. W. Tan, K. H. Tan, Y. T. Ong, A. R. Mohamed, S. H. S. Zein and S. H. Tan, *Environ. Chem. Lett.*, 2012, **10**, 265–273.
14 V. K. K. Upadhyayula, S. G. Deng, M. C. Mitchell and G. B. Smith, *Sci. Total Environ.*, 2009, **408**, 1–13.
15 Q. Zhang, J. Q. Huang, W. Z. Qian, Y. Y. Zhang and F. Wei, *Small*, 2013, **9**, 1237–1265.
16 Q. Zhang, J. Q. Huang, M. Q. Zhao, W. Z. Qian and F. Wei, *ChemSusChem*, 2011, **4**, 864–889.
17 Y. Hu, L. X. Kang, Q. C. Zhao, H. Zhong, S. C. Zhang, L. W. Yang, Z. Q. Wang, J. J. Lin, Q. W. Li, Z. Y. Zhang, L. M. Peng, Z. F. Liu and J. Zhang, *Nat. Commun.*, 2015, **6**, 6099.
18 B. L. Liu, C. Wang, J. Liu, Y. C. Che and C. W. Zhou, *Nanoscale*, 2013, **5**, 9483–9502.
19 I. Ibrahim, T. Gemming, W. M. Weber, T. Mikolajick, Z. F. Liu and M. H. Rummeli, *ACS Nano*, 2016, **10**, 7248–7266.
20 C. Liu and H. M. Cheng, *J. Am. Chem. Soc.*, 2016, **138**, 6690–6698.
21 F. Yang, X. Wang, M. H. Li, X. Y. Liu, X. L. Zhao, D. Q. Zhang, Y. Zhang, J. Yang and Y. Li, *Acc. Chem. Res.*, 2016, **49**, 606–615.
22 B. L. Liu, F. Q. Wu, H. Gui, M. Zheng and C. W. Zhou, *ACS Nano*, 2017, **11**, 31–53.
23 R. F. Zhang, Y. Y. Zhang and F. Wei, *Chem. Soc. Rev.*, 2017, **46**, 3661–3715.
24 R. F. Zhang, Y. Y. Zhang and F. Wei, *Acc. Chem. Res.*, 2017, **50**, 179–189.
25 J. K. Holt, H. G. Park, Y. M. Wang, M. Stadermann, A. B. Artyukhin, C. P. Grigoropoulos, A. Noy and O. Bakajin, *Science*, 2006, **312**, 1034–1037.
26 D. N. Futaba, K. Hata, T. Yamada, T. Hiraoka, Y. Hayamizu, Y. Kakudate, O. Tanaike, H. Hatori, M. Yumura and S. Iijima, *Nat. Mater.*, 2006, **5**, 987–994.
27 W. Lu, L. T. Qu, K. Henry and L. M. Dai, *J. Power Sources*, 2009, **189**, 1270–1277.
28 S. Esconjauregui, M. Fouquet, B. C. Bayer, C. Ducati, R. Smajda, S. Hofmann and J. Robertson, *ACS Nano*, 2010, **4**, 7431–7436.
29 N. Perea-Lopez, B. Rebollo-Plata, J. A. Briones-Leon, A. Morelos-Gomez, D. Hernandez-Cruz, G. A. Hirata, V. Meunier, A. R. Botello-Mendez, J. C. Charlier, B. Maruyama, E. Munoz-Sandoval, F. Lopez-Urias, M. Terrones and H. Terrones, *ACS Nano*, 2011, **5**, 5072–5077.
30 L. T. Qu, L. M. Dai, M. Stone, Z. H. Xia and Z. L. Wang, *Science*, 2008, **322**, 238–242.

31 B. L. Wardle, D. S. Saito, E. J. Garcia, A. J. Hart, R. G. de Villoria and E. A. Verploegen, *Adv. Mater.*, 2008, **20**, 2707–2714.
32 A. Brieland-Shoultz, S. Tawfick, S. J. Park, M. Bedewy, M. R. Maschmann, J. W. Baur and A. J. Hart, *Adv. Funct. Mater.*, 2014, **24**, 5728–5735.
33 B. J. Hinds, N. Chopra, T. Rantell, R. Andrews, V. Gavalas and L. G. Bachas, *Science*, 2004, **303**, 62–65.
34 N. Bui, E. R. Meshot, S. Kim, J. Pena, P. W. Gibson, K. J. Wu and F. Fornasiero, *Adv. Mater.*, 2016, **28**, 5871–5877.
35 K. L. Jiang, J. P. Wang, Q. Q. Li, L. A. Liu, C. H. Liu and S. S. Fan, *Adv. Mater.*, 2011, **23**, 1154–1161.
36 K. Mizuno, J. Ishii, H. Kishida, Y. Hayamizu, S. Yasuda, D. N. Futaba, M. Yumura and K. Hata, *Proc. Natl. Acad. Sci. U. S. A.*, 2009, **106**, 6044–6047.
37 S. Kim, H. Sojoudi, H. Zhao, D. Mariappan, G. H. McKinley, K. K. Gleason and A. J. Hart, *Sci. Adv.*, 2016, **2**, e1601660.
38 A. Sharma, V. Singh, T. L. Bougher and B. A. Cola, *Nat. Nanotechnol.*, 2015, **10**, 1027–1032.
39 W. Choi, S. Hong, J. T. Abrahamson, J. H. Han, C. Song, N. Nair, S. Baik and M. S. Strano, *Nat. Mater.*, 2010, **9**, 423–429.
40 Y. T. Yeh, Y. Tang, A. Sebastian, A. Dasgupta, N. Perea-Lopez, I. Albert, H. G. Lu, M. Terrones and S. Y. Zheng, *Sci. Adv.*, 2016, **2**, e1601026.
41 H. X. Chang and H. K. Wu, *Energy Environ. Sci.*, 2013, **6**, 3483–3507.
42 K. C. Kemp, H. Seema, M. Saleh, N. H. Le, K. Mahesh, V. Chandra and K. S. Kim, *Nanoscale*, 2013, **5**, 3149–3171.
43 S. Nardecchia, D. Carriazo, M. L. Ferrer, M. C. Gutierrez and F. del Monte, *Chem. Soc. Rev.*, 2013, **42**, 794–830.
44 F. Perreault, A. F. de Faria and M. Elimelech, *Chem. Soc. Rev.*, 2015, **44**, 5861–5896.
45 Y. Shen, Q. L. Fang and B. L. Chen, *Environ. Sci. Technol.*, 2015, **49**, 67–84.
46 Z. Y. Wang and B. X. Mi, *Environ. Sci. Technol.*, 2017, **51**, 8229–8244.
47 Q. B. Yun, Q. P. Lu, X. Zhang, C. L. Tan and H. Zhang, *Angew. Chem., Int. Ed.*, 2018, **57**, 626–646.
48 H. Zhang, J. Nai, L. Yu and X. W. Lou, *Joule*, 2017, **1**, 77–107.
49 L. M. Gilbertson, J. B. Zimmerman, D. L. Plata, J. E. Hutchison and P. T. Anastas, *Chem. Soc. Rev.*, 2015, **44**, 5758–5777.
50 M. L. Healy, L. J. Dahlben and J. A. Isaacs, *J. Ind. Ecol.*, 2008, **12**, 376–393.
51 D. Kushnir and B. A. Sanden, *J. Ind. Ecol.*, 2008, **12**, 360–375.
52 O. G. Griffiths, J. P. O'Byrne, L. Torrente-Murciano, M. D. Jones, D. Mattia and M. C. McManus, *J. Cleaner Prod.*, 2013, **42**, 180–189.
53 B. Mossman, W. Light and E. Wei, *Annu. Rev. Pharmacol.*, 1983, **23**, 595–615.
54 L. N. Vandenberg, R. Hauser, M. Marcus, N. Olea and W. V. Welshons, *Reprod. Toxicol.*, 2007, **24**, 139–177.
55 P. J. Squillace, J. S. Zogorski, W. G. Wilber and C. V. Price, *Environ. Sci. Technol.*, 1996, **30**, 1721–1730.
56 D. L. Plata, A. J. Hart, C. M. Reddy and P. M. Gschwend, *Environ. Sci. Technol.*, 2009, **43**, 8367–8373.
57 M. J. Eckelman, M. S. Mauter, J. A. Isaacs and M. Elimelech, *Environ. Sci. Technol.*, 2012, **46**, 2902–2910.
58 D. L. Plata, E. R. Meshot, C. M. Reddy, A. J. Hart and P. M. Gschwend, *ACS Nano*, 2010, **4**, 7185–7192.
59 D. Y. Kim, H. Sugime, K. Hasegawa, T. Osawa and S. Noda, *Carbon*, 2011, **49**, 1972–1979.
60 C. F. Wu, M. A. Nahil, N. Miskolczi, J. Huang and P. T. Williams, *Environ. Sci. Technol.*, 2014, **48**, 819–826.
61 A. F. Trompeta, M. A. Koklioti, D. K. Perivoliotis, I. Lynch and C. A. Charitidis, *J. Cleaner Prod.*, 2016, **129**, 384–394.
62 P. Zhai, J. A. Isaacs and M. J. Eckelman, *Appl. Energy*, 2016, **173**, 624–634.
63 S. Licht, A. Douglas, J. W. Ren, R. Carter, M. Lefler and C. L. Pint, *ACS Cent. Sci.*, 2016, **2**, 162–168.
64 H. Almkhelfe, J. Carpena-Nunez, T. C. Back and P. B. Amama, *Nanoscale*, 2016, **8**, 13476–13487.
65 I. A. Martorell, W. D. Partlow, R. M. Young, J. J. Schreurs and H. E. Saunders, *Diamond Relat. Mater.*, 1999, **8**, 29–36.
66 M. J. Bronikowski, P. A. Willis, D. T. Colbert, K. A. Smith and R. E. Smalley, *J. Vac. Sci. Technol., A*, 2001, **19**, 1800–1805.
67 A. E. Agboola, R. W. Pike, T. A. Hertwig and H. H. Lou, *Clean Technol. Environ.*, 2007, **9**, 289–311.
68 S. S. Meysami, L. C. Snoek and N. Grobert, *Anal. Chem.*, 2014, **86**, 8850–8856.
69 M. Cantoro, S. Hofmann, S. Pisana, V. Scardaci, A. Parvez, C. Ducati, A. C. Ferrari, A. M. Blackburn, K. Y. Wang and J. Robertson, *Nano Lett.*, 2006, **6**, 1107–1112.
70 S. Hofmann, C. Ducati, J. Robertson and B. Kleinsorge, *Appl. Phys. Lett.*, 2003, **83**, 135–137.
71 G. D. Nessim, M. Seita, K. P. O'Brien, A. J. Hart, R. K. Bonaparte, R. R. Mitchell and C. V. Thompson, *Nano Lett.*, 2009, **9**, 3398–3405.
72 A. Magrez, J. W. Seo, R. Smajda, B. Korbely, J. C. Andresen, M. Mionic, S. Casimirius and L. Forro, *ACS Nano*, 2010, **4**, 3702–3708.
73 S. Yasuda, D. N. Futaba, T. Yamada, J. Satou, A. Shibuya, H. Takai, K. Arakawa, M. Yumura and K. Hata, *ACS Nano*, 2009, **3**, 4164–4170.
74 R. G. de Villoria, A. J. Hart and B. L. Wardle, *ACS Nano*, 2011, **5**, 4850–4857.
75 K. Hata, D. N. Futaba, K. Mizuno, T. Namai, M. Yumura and S. Iijima, *Science*, 2004, **306**, 1362–1364.
76 D. N. Futaba, K. Hata, T. Yamada, K. Mizuno, M. Yumura and S. Iijima, *Phys. Rev. Lett.*, 2005, **95**, 056104.
77 M. Bystrzejewski, R. Schonfelder, G. Cuniberti, H. Lange, A. Huczko, T. Gemming, T. Pichler, B. Buchner and M. Rummeli, *Chem. Mater.*, 2008, **20**, 6586–6588.
78 C. L. Pint, S. T. Pheasant, A. N. G. Parra-Vasquez, C. Horton, Y. Q. Xu and R. H. Hauge, *J. Phys. Chem. C*, 2009, **113**, 4125–4133.

79 K. Hasegawa and S. Noda, *ACS Nano*, 2011, **5**, 975–984.
80 R. M. Wyss, J. E. Klare, H. G. Park, A. Noy, O. Bakajin and V. Lulevich, *ACS Appl. Mater. Interfaces*, 2014, **6**, 21019–21025.
81 G. Y. Zhang, D. Mann, L. Zhang, A. Javey, Y. M. Li, E. Yenilmez, Q. Wang, J. P. McVittie, Y. Nishi, J. Gibbons and H. J. Dai, *Proc. Natl. Acad. Sci. U. S. A.*, 2005, **102**, 16141–16145.
82 G. D. Nessim, A. Al-Obeidi, H. Grisaru, E. S. Polsen, C. R. Oliver, T. Zimrin, A. J. Hart, D. Aurbach and C. V. Thompson, *Carbon*, 2012, **50**, 4002–4009.
83 Z. J. Ruan, W. H. Rong, Q. Q. Li and Z. Li, *Carbon*, 2015, **87**, 338–346.
84 W. B. Shi, J. J. Li, E. S. Polsen, C. R. Oliver, Y. K. Zhao, E. R. Meshot, M. Barclay, D. H. Fairbrother, A. J. Hart and D. L. Plata, *Nanoscale*, 2017, **9**, 5222–5233.
85 I. V. Anoshkin, A. G. Nasibulin, Y. Tian, B. Liu, H. Jiang and E. I. Kauppinen, *Carbon*, 2014, **78**, 130–136.
86 R. Xiang, E. Einarsson, J. Okawa, Y. Miyauchi and S. Maruyama, *J. Phys. Chem. C*, 2009, **113**, 7511–7515.
87 Y. Y. Zhang, J. M. Gregoire, R. B. van Dover and A. J. Hart, *J. Phys. Chem. C*, 2010, **114**, 6389–6395.
88 Q. Wen, W. Z. Qian, F. Wei, Y. Liu, G. Q. Ning and Q. Zhang, *Chem. Mater.*, 2007, **19**, 1226–1230.
89 Z. R. Li, Y. Xu, X. D. Ma, E. Dervishi, V. Saini, A. R. Biris, D. Lupu and A. S. Biris, *Chem. Commun.*, 2008, 3260–3262, DOI: 10.1039/b803465f.
90 D. N. Futaba, J. Goto, S. Yasuda, T. Yamada, M. Yumura and K. Hata, *Adv. Mater.*, 2009, **21**, 4811–4815.
91 A. Douglas, R. Carter, N. Muralidharan, L. Oakes and C. L. Pint, *Carbon*, 2017, **116**, 572–578.
92 H. Almkhelfe, X. Li, R. Rao and P. B. Amama, *Carbon*, 2017, **116**, 181–190.
93 Z. Spitalsky, D. Tasis, K. Papagelis and C. Galiotis, *Prog. Polym. Sci.*, 2010, **35**, 357–401.
94 D. Eder, *Chem. Rev.*, 2010, **110**, 1348–1385.
95 J. C. Li, P. X. Hou and C. Liu, *Small*, 2017, **13**, 1702002.
96 M. De Volder, S. H. Tawfick, S. J. Park, D. Copic, Z. Z. Zhao, W. Lu and A. J. Hart, *Adv. Mater.*, 2010, **22**, 4384–4389.
97 S. Kim, F. Fornasiero, H. G. Park, J. Bin In, E. Meshot, G. Giraldo, M. Stadermann, M. Fireman, J. Shan, C. P. Grigoropoulos and O. Bakajin, *J. Membr. Sci.*, 2014, **460**, 91–98.
98 W. L. Mi, Y. S. Lin and Y. D. Li, *J. Membr. Sci.*, 2007, **304**, 1–7.
99 F. Du, L. T. Qu, Z. H. Xia, L. F. Feng and L. M. Dai, *Langmuir*, 2011, **27**, 8437–8443.
100 B. Lee, Y. Baek, M. Lee, D. H. Jeong, H. H. Lee, J. Yoon and Y. H. Kim, *Nat. Commun.*, 2015, **6**, 7109.
101 M. E. Alf, A. Asatekin, M. C. Barr, S. H. Baxamusa, H. Chelawat, G. Ozaydin-Ince, C. D. Petruczok, R. Sreenivasan, W. E. Tenhaeff, N. J. Trujillo, S. Vaddiraju, J. J. Xu and K. K. Gleason, *Adv. Mater.*, 2010, **22**, 1993–2027.
102 K. K. S. Lau, J. Bico, K. B. K. Teo, M. Chhowalla, G. A. J. Amaratunga, W. I. Milne, G. H. McKinley and K. K. Gleason, *Nano Lett.*, 2003, **3**, 1701–1705.
103 H. Zhang, G. P. Cao, Z. Y. Wang, Y. S. Yang, Z. J. Shi and Z. N. Gu, *Nano Lett.*, 2008, **8**, 2664–2668.
104 Z. Yang, X. M. Zhou, Z. P. Jin, Z. Liu, H. G. Nie, X. A. Chen and S. M. Huang, *Adv. Mater.*, 2014, **26**, 3156–3161.
105 J. Y. Cheng, B. Zhao, W. K. Zhang, F. Shi, G. P. Zheng, D. Q. Zhang and J. H. Yang, *Adv. Funct. Mater.*, 2015, **25**, 7381–7391.
106 W. K. Zhang, B. Zhao, Y. L. Yin, T. Yin, J. Y. Cheng, K. Zhan, Y. Yan, J. H. Yang and J. Q. Li, *J. Mater. Chem. A*, 2016, **4**, 19026–19036.
107 H. B. Zhao, C. Jacob, H. A. Stone and A. J. Hart, *Langmuir*, 2016, **32**, 12686–12692.
108 L. Acauan, A. C. Dias, M. B. Pereira, F. Horowitz and C. P. Bergmann, *ACS Appl. Mater. Interfaces*, 2016, **8**, 16444–16450.
109 S. M. George, *Chem. Rev.*, 2010, **110**, 111–131.
110 F. Du, D. S. Yu, L. M. Dai, S. Ganguli, V. Varshney and A. K. Roy, *Chem. Mater.*, 2011, **23**, 4810–4816.
111 R. V. Salvatierra, D. Zakhidov, J. W. Sha, N. D. Kim, S. K. Lee, A. R. O. Raji, N. Q. Zhao and J. M. Tour, *ACS Nano*, 2017, **11**, 2724–2733.
112 C. G. Hu and L. M. Dai, *Angew. Chem., Int. Ed.*, 2016, **55**, 11736–11758.
113 X. Liu and L. M. Dai, *Nat. Rev. Mater.*, 2016, **1**, 16064.
114 K. P. Gong, F. Du, Z. H. Xia, M. Durstock and L. M. Dai, *Science*, 2009, **323**, 760–764.
115 W. Xiong, F. Du, Y. Liu, A. Perez, M. Supp, T. S. Ramakrishnan, L. M. Dai and L. Jiang, *J. Am. Chem. Soc.*, 2010, **132**, 15839–15841.
116 P. P. Sharma, J. J. Wu, R. M. Yadav, M. J. Liu, C. J. Wright, C. S. Tiwary, B. I. Yakobson, J. Lou, P. M. Ajayan and X. D. Zhou, *Angew. Chem., Int. Ed.*, 2015, **54**, 13701–13705.
117 X. Q. Wang, J. S. Lee, Q. Zhu, J. Liu, Y. Wang and S. Dai, *Chem. Mater.*, 2010, **22**, 2178–2180.
118 Y. Liu, Y. T. Shen, L. T. Sun, J. C. Li, C. Liu, W. C. Ren, F. Li, L. B. Gao, J. Chen, F. C. Liu, Y. Y. Sun, N. J. Tang, H. M. Cheng and Y. W. Du, *Nat. Commun.*, 2016, **7**, 10921.
119 D. S. Yu, Q. Zhang and L. M. Dai, *J. Am. Chem. Soc.*, 2010, **132**, 15127–15129.
120 Y. Wang, Y. Y. Shao, D. W. Matson, J. H. Li and Y. H. Lin, *ACS Nano*, 2010, **4**, 1790–1798.
121 H. M. Jeong, J. W. Lee, W. H. Shin, Y. J. Choi, H. J. Shin, J. K. Kang and J. W. Choi, *Nano Lett.*, 2011, **11**, 2472–2477.
122 G. Singh, D. S. Sutar, V. D. Botcha, P. K. Narayanam, S. S. Talwar, R. S. Srinivasa and S. S. Major, *Nanotechnology*, 2013, **24**, 355704.
123 K. R. Zodrow, Q. L. Li, R. M. Buono, W. Chen, G. Daigger, L. Duenas-Osorio, M. Elimelech, X. Huang, G. B. Jiang, J. H. Kim, B. E. Logan, D. L. Sedlak, P. Westerhoff and P. J. J. Alvarez, *Environ. Sci. Technol.*, 2017, **51**, 10274–10281.
124 S. Agnihotri, J. P. B. Mota, M. Rostam-Abadi and M. J. Rood, *J. Phys. Chem. B*, 2006, **110**, 7640–7647.

125 B. Pan and B. S. Xing, *Environ. Sci. Technol.*, 2008, **42**, 9005–9013.
126 D. Zilli, P. R. Bonelli and A. L. Cukierman, *Nanotechnology*, 2006, **17**, 5136–5141.
127 R. Q. Long and R. T. Yang, *Ind. Eng. Chem. Res.*, 2001, **40**, 4288–4291.
128 F. Sun, J. H. Gao, Y. W. Zhu, G. Q. Chen, S. H. Wu and Y. K. Qin, *Adsorption*, 2013, **19**, 959–966.
129 S. Agnihotri, M. J. Rood and M. Rostam-Abadi, *Carbon*, 2005, **43**, 2379–2388.
130 R. Q. Long and R. T. Yang, *J. Am. Chem. Soc.*, 2001, **123**, 2058–2059.
131 P. Kondratyuk, Y. Wang, J. K. Johnson and J. T. Yates, *J. Phys. Chem. B*, 2005, **109**, 20999–21005.
132 F. S. Su, C. S. Lu, W. F. Cnen, H. L. Bai and J. F. Hwang, *Sci. Total Environ.*, 2009, **407**, 3017–3023.
133 A. E. Creamer and B. Gao, *Environ. Sci. Technol.*, 2016, **50**, 7276–7289.
134 M. Cinke, J. Li, C. W. Bauschlicher, A. Ricca and M. Meyyappan, *Chem. Phys. Lett.*, 2003, **376**, 761–766.
135 D. J. Babu, M. Lange, G. Cherkashinin, A. Issanin, R. Staudt and J. J. Schneider, *Carbon*, 2013, **61**, 616–623.
136 D. P. Cao, X. R. Zhang, J. F. Chen, W. C. Wang and J. Yun, *J. Phys. Chem. B*, 2003, **107**, 13286–13292.
137 W. J. Wang, X. Peng and D. P. Cao, *Environ. Sci. Technol.*, 2011, **45**, 4832–4838.
138 M. Rahimi, J. K. Singh, D. J. Babu, J. J. Schneider and F. Muller-Plathe, *J. Phys. Chem. C*, 2013, **117**, 13492–13501.
139 M. Rahimi, D. J. Babu, J. K. Singh, Y. B. Yang, J. J. Schneider and F. Muller-Plathe, *J. Chem. Phys.*, 2015, **143**, 124701.
140 M. Rahimi, J. K. Singh and F. Muller-Plathe, *Phys. Chem. Chem. Phys.*, 2016, **18**, 4112–4120.
141 Y. B. Yang, M. Rahimi, J. K. Singh, M. C. Bohm and F. Muller-Plathe, *J. Phys. Chem. C*, 2016, **120**, 7510–7521.
142 A. C. Dillon, K. M. Jones, T. A. Bekkedahl, C. H. Kiang, D. S. Bethune and M. J. Heben, *Nature*, 1997, **386**, 377–379.
143 C. Liu, Y. Y. Fan, M. Liu, H. T. Cong, H. M. Cheng and M. S. Dresselhaus, *Science*, 1999, **286**, 1127–1129.
144 A. Y. Cao, H. W. Zhu, X. F. Zhang, X. S. Li, D. B. Ruan, C. L. Xu, B. Q. Wei, J. Liang and D. H. Wu, *Chem. Phys. Lett.*, 2001, **342**, 510–514.
145 C. Liu, Y. Chen, C. Z. Wu, S. T. Xu and H. M. Cheng, *Carbon*, 2010, **48**, 452–455.
146 X. C. Gui, J. Q. Wei, K. L. Wang, A. Y. Cao, H. W. Zhu, Y. Jia, Q. K. Shu and D. H. Wu, *Adv. Mater.*, 2010, **22**, 617–621.
147 D. P. Hashim, N. T. Narayanan, J. M. Romo-Herrera, D. A. Cullen, M. G. Hahm, P. Lezzi, J. R. Suttle, D. Kelkhoff, E. Munoz-Sandoval, S. Ganguli, A. K. Roy, D. J. Smith, R. Vajtai, B. G. Sumpter, V. Meunier, H. Terrones, M. Terrones and P. M. Ajayan, *Sci. Rep.*, 2012, **2**, 363.
148 W. Chen, L. Duan and D. Q. Zhu, *Environ. Sci. Technol.*, 2007, **41**, 8295–8300.
149 K. Yang, W. Wu, Q. Jing and L. Zhu, *Environ. Sci. Technol.*, 2008, **42**, 7931–7936.
150 S. Gotovac, H. Honda, Y. Hattori, K. Takahashi, H. Kanoh and K. Kaneko, *Nano Lett.*, 2007, **7**, 583–587.
151 X. L. Wang, S. Tao and B. S. Xing, *Environ. Sci. Technol.*, 2009, **43**, 6214–6219.
152 H. B. Li, X. C. Gui, L. H. Zhang, S. S. Wang, C. Y. Ji, J. Q. Wei, K. L. Wang, H. W. Zhu, D. H. Wu and A. Y. Cao, *Chem. Commun.*, 2010, **46**, 7966–7968.
153 F. S. Su and C. S. Lu, *J. Environ. Sci. Health, Part A: Toxic/Hazard. Subst. Environ. Eng.*, 2007, **42**, 1543–1552.
154 X. J. Zhou, X. D. Li, S. X. Xu, X. Y. Zhao, M. J. Ni and K. F. Cen, *Environ. Sci. Pollut. Res.*, 2015, **22**, 10463–10470.
155 D. Desai, E. S. Beh, S. Sahu, V. Vedharathinam, Q. van Overmeere, C. F. de Lannoy, A. P. Jose, A. R. Völkel and J. B. Rivest, *ACS Energy Lett.*, 2017, 375–379, DOI: 10.1021/acsenergylett.7b01220.
156 B. Shapira, I. Cohen, T. R. Penki, E. Avraham and D. Aurbach, *J. Power Sources*, 2018, **378**, 146–152.
157 Y. H. Li, S. G. Wang, J. Q. Wei, X. F. Zhang, C. L. Xu, Z. K. Luan, D. H. Wu and B. Q. Wei, *Chem. Phys. Lett.*, 2002, **357**, 263–266.
158 Y. H. Li, S. G. Wang, Z. K. Luan, J. Ding, C. L. Xu and D. H. Wu, *Carbon*, 2003, **41**, 1057–1062.
159 Y. H. Li, Z. C. Di, J. Ding, D. H. Wu, Z. K. Luan and Y. Q. Zhu, *Water Res.*, 2005, **39**, 605–609.
160 G. P. Rao, C. Lu and F. Su, *Sep. Purif. Technol.*, 2007, **58**, 224–231.
161 Z. M. Gao, T. J. Bandosz, Z. B. Zhao, M. Han and J. S. Qiu, *J. Hazard. Mater.*, 2009, **167**, 357–365.
162 X. Y. Yu, T. Luo, Y. X. Zhang, Y. Jia, B. J. Zhu, X. C. Fu, J. H. Liu and X. J. Huang, *ACS Appl. Mater. Interfaces*, 2011, **3**, 2585–2593.
163 Y. Zhou, M. Ghaffari, M. Lin, E. M. Parsons, Y. Liu, B. L. Wardle and Q. M. Zhang, *Electrochim. Acta*, 2013, **111**, 608–613.
164 J. Chen, Y. Liu, A. I. Minett, C. Lynam, J. Z. Wang and G. G. Wallace, *Chem. Mater.*, 2007, **19**, 3595–3597.
165 A. L. M. Reddy, M. M. Shaijumon, S. R. Gowda and P. M. Ajayan, *Nano Lett.*, 2009, **9**, 1002–1006.
166 E. Frackowiak and F. Beguin, *Carbon*, 2002, **40**, 1775–1787.
167 J. W. Liu, J. Essner and J. Li, *Chem. Mater.*, 2010, **22**, 5022–5030.
168 X. W. Cui, F. P. Hu, W. F. Wei and W. X. Chen, *Carbon*, 2011, **49**, 1225–1234.
169 Y. Q. Jiang, P. B. Wang, X. N. Zang, Y. Yang, A. Kozinda and L. W. Lin, *Nano Lett.*, 2013, **13**, 3524–3530.
170 C. Y. Jung, T. S. Zhao, L. Zeng and P. Tan, *J. Power Sources*, 2016, **331**, 82–90.
171 Y. B. Yan, J. W. Miao, Z. H. Yang, F. X. Xiao, H. B. Yang, B. Liu and Y. H. Yang, *Chem. Soc. Rev.*, 2015, **44**, 3295–3346.

172 G. Wu, A. Santandreu, W. Kellogg, S. Gupta, O. Ogoke, H. G. Zhang, H. L. Wang and L. M. Dai, *Nano Energy*, 2016, **29**, 83–110.
173 O. Akhavan, M. Abdolahad, Y. Abdi and S. Mohajerzadeh, *Carbon*, 2009, **47**, 3280–3287.
174 Y. D. Yang, L. T. Qu, L. M. Dai, T. S. Kang and M. Durstock, *Adv. Mater.*, 2007, **19**, 1239–1243.
175 H. Li, X. Gui, C. Ji, P. Li, Z. Li, L. Zhang, E. Shi, K. Zhu, J. Wei, K. Wang, H. Zhu, D. Wu and A. Cao, *Nano Res.*, 2012, **5**, 265–271.
176 W. J. Lee, J. M. Lee, S. T. Kochuveedu, T. H. Han, H. Y. Jeong, M. Park, J. M. Yun, J. Kwon, K. No, D. H. Kim and S. O. Kim, *ACS Nano*, 2012, **6**, 935–943.
177 H. A. Park, S. Y. Liu, Y. Oh, P. A. Salvador, G. S. Rohrer and M. F. Islam, *ACS Nano*, 2017, **11**, 2150–2159.
178 J. E. Mink, J. P. Rojas, B. E. Logan and M. M. Hussain, *Nano Lett.*, 2012, **12**, 791–795.
179 L. Xiang, P. Yu, M. N. Zhang, J. Hao, Y. X. Wang, L. Zhu, L. M. Dai and L. Q. Mao, *Anal. Chem.*, 2014, **86**, 5017–5023.
180 S. Y. Wang, E. Iyyamperumal, A. Roy, Y. H. Xue, D. S. Yu and L. M. Dai, *Angew. Chem., Int. Ed.*, 2011, **50**, 11756–11760.
181 D. J. Li, U. N. Maiti, J. Lim, D. S. Choi, W. J. Lee, Y. Oh, G. Y. Lee and S. O. Kim, *Nano Lett.*, 2014, **14**, 1228–1233.
182 X. Su, J. Wu and B. J. Hinds, *Carbon*, 2011, **49**, 1145–1150.
183 D. P. Li and J. H. Qu, *J. Environ. Sci.*, 2009, **21**, 713–719.
184 T. Tsubota, A. Ono, N. Murakami and T. Ohno, *Appl. Catal., B*, 2009, **91**, 533–538.
185 Z. Q. Liu, J. Ma, Y. H. Cui, L. Zhao and B. P. Zhang, *Appl. Catal., B*, 2010, **101**, 74–80.
186 O. Akhavan, M. Abdolahad, Y. Abdi and S. Mohajerzadeh, *J. Mater. Chem.*, 2011, **21**, 387–393.
187 G. Centi, P. Ciambelli, S. Perathoner and P. Russo, *Catal. Today*, 2002, **75**, 3–15.
188 L. S. Wang, B. C. Huang, Y. X. Su, G. Y. Zhou, K. L. Wang, H. C. Luo and D. Q. Ye, *Chem. Eng. J.*, 2012, **192**, 232–241.
189 H. J. Joung, J. H. Kim, J. S. Oh, D. W. You, H. O. Park and K. W. Jung, *Appl. Surf. Sci.*, 2014, **290**, 267–273.
190 C. H. Kuo, W. K. Li, W. Q. Song, Z. Luo, A. S. Poyraz, Y. Guo, A. W. K. Ma, S. L. Suib and J. He, *ACS Appl. Mater. Interfaces*, 2014, **6**, 11311–11317.
191 J. Han, D. S. Zhang, P. Maitarad, L. Y. Shi, S. X. Cai, H. R. Li, L. Huang and J. P. Zhang, *Catal. Sci. Technol.*, 2015, **5**, 438–446.
192 Z. P. Qu, L. Miao, H. Wang and Q. Fu, *Chem. Commun.*, 2015, **51**, 956–958.
193 B. Zhao, X. W. Liu, Z. J. Zhou, H. Z. Shao and M. H. Xu, *Chem. Eng. J.*, 2016, **284**, 1233–1241.
194 H. M. Xu, N. Q. Yan, Z. Qu, W. Liu, J. Mei, W. J. Huang and S. J. Zhao, *Environ. Sci. Technol.*, 2017, **51**, 8879–8892.
195 C. Fang, D. S. Zhang, S. X. Cai, L. Zhang, L. Huang, H. R. Li, P. Maitarad, L. Y. Shi, R. H. Gao and J. P. Zhang, *Nanoscale*, 2013, **5**, 9199–9207.
196 B. Y. Bai, J. H. Li and J. M. Hao, *Appl. Catal., B*, 2015, **164**, 241–250.
197 X. J. Fan, H. Q. Zhou and X. Guo, *ACS Nano*, 2015, **9**, 5125–5134.
198 R. Amade, M. Vila-Costa, S. Hussain, E. O. Casamayor and E. Bertran, *J. Mater. Sci.*, 2015, **50**, 1214–1220.
199 H. G. Park and Y. Jung, *Chem. Soc. Rev.*, 2014, **43**, 565–576.
200 S. R. Guo, E. R. Meshot, T. Kuykendall, S. Cabrini and F. Fornasiero, *Adv. Mater.*, 2015, **27**, 5726–5737.
201 H. Y. Yang, Z. J. Han, S. F. Yu, K. L. Pey, K. Ostrikov and R. Karnik, *Nat. Commun.*, 2013, **4**, 2220.
202 R. H. Tunuguntla, R. Y. Henley, Y. C. Yao, T. A. Pham, M. Wanunu and A. Noy, *Science*, 2017, **357**, 792–796.
203 R. Das, M. E. Ali, S. B. Abd Hamid, S. Ramakrishna and Z. Z. Chowdhury, *Desalination*, 2014, **336**, 97–109.
204 M. N. Nejad, M. Asghari and M. Afsari, *ChemBioEng Rev.*, 2016, **3**, 276–298.
205 J. Wu, K. S. Paudel, C. Strasinger, D. Hammell, A. L. Stinchcomb and B. J. Hinds, *Proc. Natl. Acad. Sci. U. S. A.*, 2010, **107**, 11698–11702.
206 F. Fornasiero, *Curr. Opin. Chem. Eng.*, 2017, **16**, 1–8.
207 G. Hummer, J. C. Rasaiah and J. P. Noworyta, *Nature*, 2001, **414**, 188–190.
208 B. Corry, *Energy Environ. Sci.*, 2011, **4**, 751–759.
209 M. Majumder, N. Chopra and B. J. Hinds, *J. Am. Chem. Soc.*, 2005, **127**, 9062–9070.
210 F. Fornasiero, H. G. Park, J. K. Holt, M. Stadermann, C. P. Grigoropoulos, A. Noy and O. Bakajin, *Proc. Natl. Acad. Sci. U. S. A.*, 2008, **105**, 17250–17255.
211 M. Majumder, A. Stinchcomb and B. J. Hinds, *Life Sci.*, 2010, **86**, 563–568.
212 J. Wu, K. Gerstandt, H. B. Zhang, J. Liu and B. J. Hinds, *Nat. Nanotechnol.*, 2012, **7**, 133–139.
213 X. H. Sun, X. Su, J. Wu and B. J. Hinds, *Langmuir*, 2011, **27**, 3150–3156.
214 D. Yoon, C. Lee, J. Yun, W. Jeon, B. J. Cha and S. Baik, *ACS Nano*, 2012, **6**, 5980–5987.
215 H. B. Chen and D. S. Sholl, *J. Membr. Sci.*, 2006, **269**, 152–160.
216 L. Ge, L. Wang, A. J. Du, M. Hou, V. Rudolph and Z. H. Zhu, *RSC Adv.*, 2012, **2**, 5329–5336.
217 S. Ban and C. Huang, *J. Membr. Sci.*, 2012, **417**, 113–118.
218 G. Arora and S. I. Sandler, *J. Chem. Phys.*, 2005, **123**, 044705.
219 K. Gethard, O. Sae-Khow and S. Mitra, *ACS Appl. Mater. Interfaces*, 2011, **3**, 110–114.
220 A. I. Skoulidas, D. M. Ackerman, J. K. Johnson and D. S. Sholl, *Phys. Rev. Lett.*, 2002, **89**, 185901.
221 S. Kim, J. R. Jinschek, H. Chen, D. S. Sholl and E. Marand, *Nano Lett.*, 2007, **7**, 2806–2811.
222 H. B. Chen and D. S. Sholl, *J. Am. Chem. Soc.*, 2004, **126**, 7778–7779.
223 Z. Yin, H. Wang, M. Jian, Y. Li, K. Xia, M. Zhang, C. Wang, Q. Wang, M. Ma, Q.-S. Zheng and Y. Zhang, *ACS Appl. Mater. Interfaces*, 2017, **9**, 28596–28603.
224 J. K. Holt, A. Noy, T. Huser, D. Eaglesham and O. Bakajin, *Nano Lett.*, 2004, **4**, 2245–2250.

225 M. Majumder, N. Chopra and B. J. Hinds, *ACS Nano*, 2011, **5**, 3867–3877.
226 K. J. Lee and H. D. Park, *J. Membr. Sci.*, 2016, **501**, 144–151.
227 Y. Baek, C. Kim, D. K. Seo, T. Kim, J. S. Lee, Y. H. Kim, K. H. Ahn, S. S. Bae, S. C. Lee, J. Lim, K. Lee and J. Yoon, *J. Membr. Sci.*, 2014, **460**, 171–177.
228 M. Yu, H. H. Funke, J. L. Falconer and R. D. Noble, *Nano Lett.*, 2009, **9**, 225–229.
229 N. Yang, M. Li, J. Patscheider, S. K. Youn and H. G. Park, *Sci. Rep.*, 2017, **7**, 46725.
230 B. Corry, *J. Phys. Chem. B*, 2008, **112**, 1427–1434.
231 H. K. Mutha, Y. Lu, I. Y. Stein, H. J. Cho, M. E. Suss, T. Laoui, C. V. Thompson, B. L. Wardle and E. N. Wang, *Nanotechnology*, 2017, **28**, 05LT01.
232 E. R. Meshot, D. W. Zwissler, N. Bui, T. R. Kuykendall, C. Wang, A. Hexerner, K. J. J. Wu and F. Fornasiero, *ACS Nano*, 2017, **11**, 5405–5416.
233 E. R. Meshot, D. L. Plata, S. Tawfick, Y. Y. Zhang, E. A. Verploegen and A. J. Hart, *ACS Nano*, 2009, **3**, 2477–2486.
234 E. S. Polsen, M. Bedewy and A. J. Hart, *Small*, 2013, **9**, 2564–2575.
235 M. Wang, T. T. Li, Y. G. Yao, H. F. Lu, Q. Li, M. H. Chen and Q. W. Li, *J. Am. Chem. Soc.*, 2014, **136**, 18156–18162.
236 H. Sojoudi, S. Kim, H. Zhao, R. K. Annavarapu, D. Mariappan, A. J. Hart, G. H. McKinley and K. K. Gleason, *ACS Appl. Mater. Interfaces*, 2017, **9**, 43287–43299.
237 V. K. K. Upadhyayula, D. E. Meyer, M. A. Curran and M. A. Gonzalez, *J. Cleaner Prod.*, 2012, **26**, 37–47.
238 L. J. Dahlben, M. J. Eckelman, A. Hakimian, S. Somu and J. A. Isaacs, *Environ. Sci. Technol.*, 2013, **47**, 8471–8478.
239 L. M. Gilbertson, A. A. Busnaina, J. A. Isaacs, J. B. Zimmerman and M. J. Eckelman, *Environ. Sci. Technol.*, 2014, **48**, 11360–11368.

